SUPPORTING INFORMATION

Enhancement of gold catalytic activity and stability by immobilization on the surface of graphene

David Ventura-Espinosa, Sara Sabater and Jose A. Mata*

Institute of Advanced Materials (INAM), Universitat Jaume I. Avda. Sos Baynat s/n, 12006, Castellón (Spain). e-mail: jmata@uji.es

Contents

S1. Catalytic experiments

Table S1: Optimization parameters for the intramolecular hydroamination of alkynes.

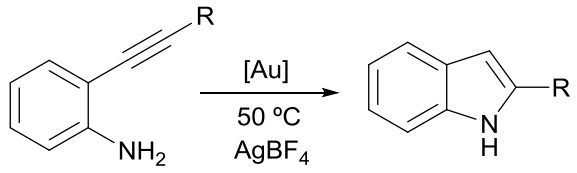

Entry	Catalyst	[Au] (mol %)	R	Solvent	Time (h)	Yield (%)[a]
1	**-**	-	Ph	Toluene	6	0
2[b]	**-**	-	Ph	"	6	0
3	**rGO**	-	Ph	"	6	0
4	**3**	1	Ph	"	6	20
5	**3**	1	nBu	"	8	32
6	**3**	1	nBu	"	24	40
7	**4**	1	nBu	"	8	50
8	**4**	1	nBu	"	24	71(65)
9	**4**	1	Ph	"	6	91
10	**4**	1	Ph	"	24	100(92)
11[c]	**4**	1	Ph	"	6	71
12[c]	**4**	1	Ph	"	24	100
13	**4**	2	Ph	"	1	100(90)
14[d]	**4**	2	Ph	"	1	100
15	**4**	2	Ph	THF	6	15
16	**4**	2	Ph	MeCN	1	100
17	**5**	1	Ph	Toluene	6	82
18	**6**	0.08	Ph	Toluene	1.5	100
19	**6**	0.08	Ph	MeCN	24	93
20	**6**	0.56	Ph	Toluene	12 min	100

[a] Reactions carried out at a substrate concentration of 0.0625M. Yields determined by GC analysis using anisole as the internal standard. Three equivalents of $AgBF_4$ respect to gold catalyst. Isolated yields in parenthesis. See section S2.4 for characterization. [b] Reaction carried out in the presence of 6 mol % of $AgBF_4$. [c] Reactions carried out at a substrate concentration of 0.03125M. [d] Reaction carried out under N_2 atmosphere.

S2. Nuclear Magnetic Resonance (NMR) Analysis

S2.1 ^{1}H NMR and $^{13}C\{^{1}H\}$ spectra of the imidazolium salt **2** in CD_2Cl_2

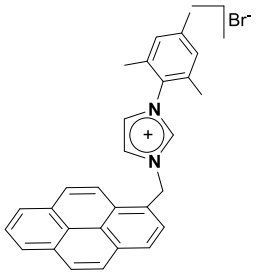

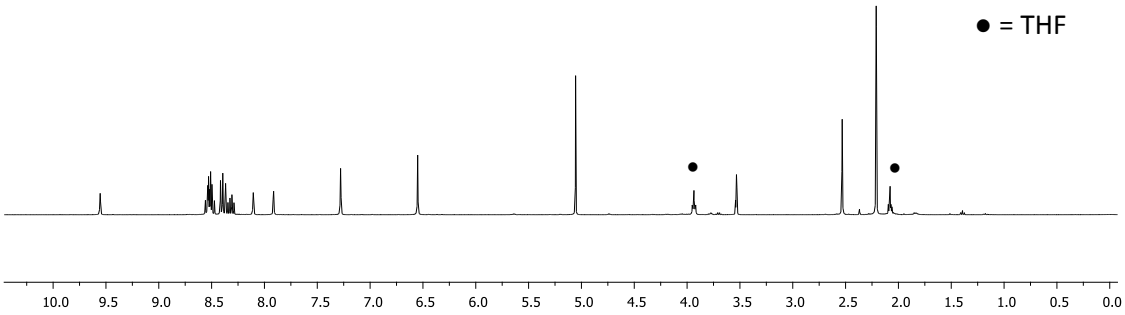

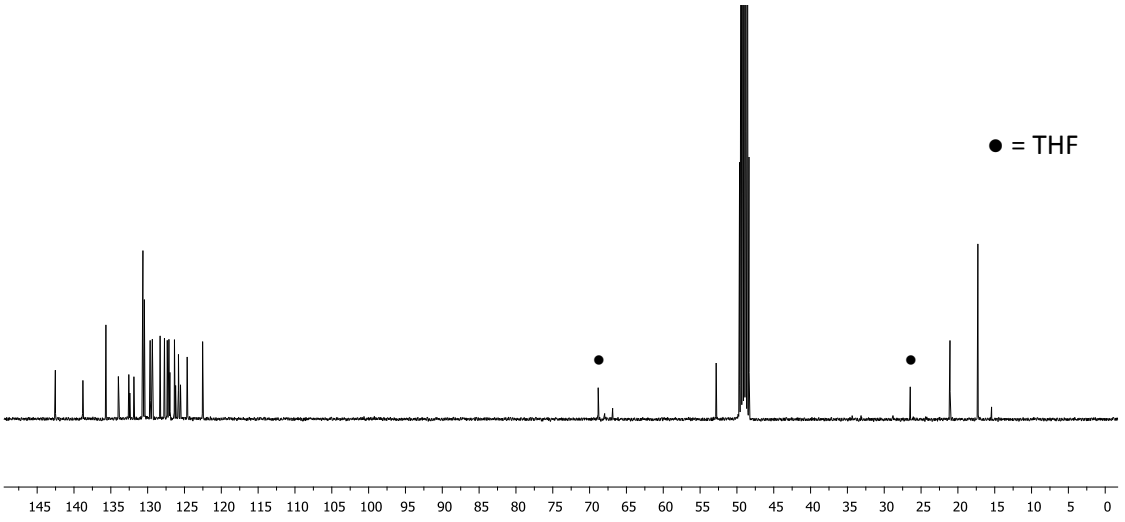

S2.2 ^{1}H NMR and $^{13}C\{^{1}H\}$ spectra of complex **3** in $CDCl_3$

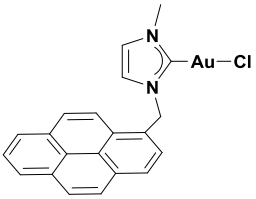

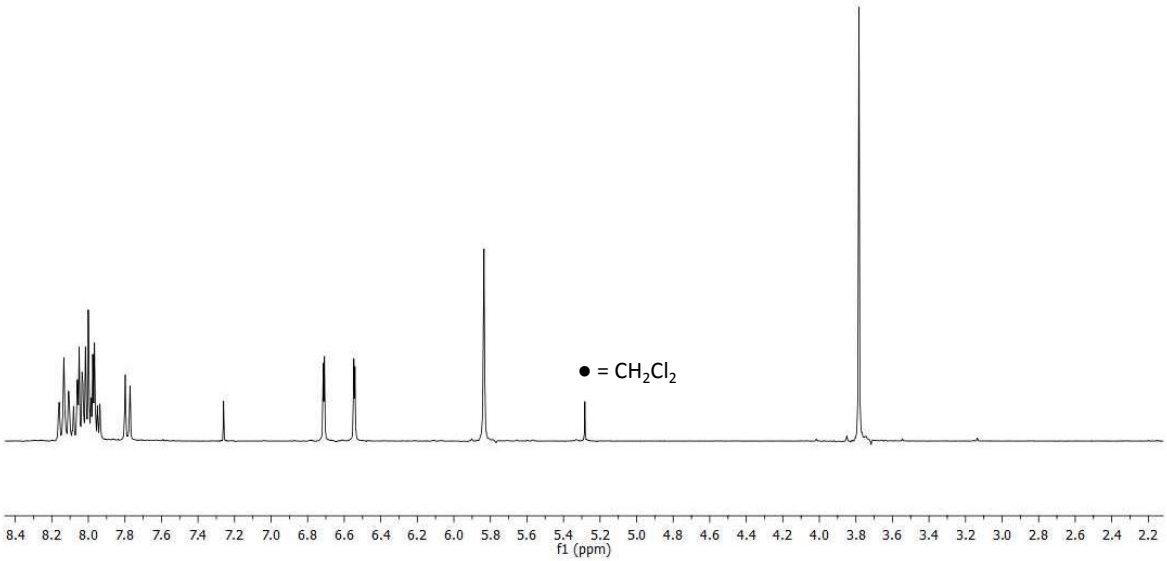

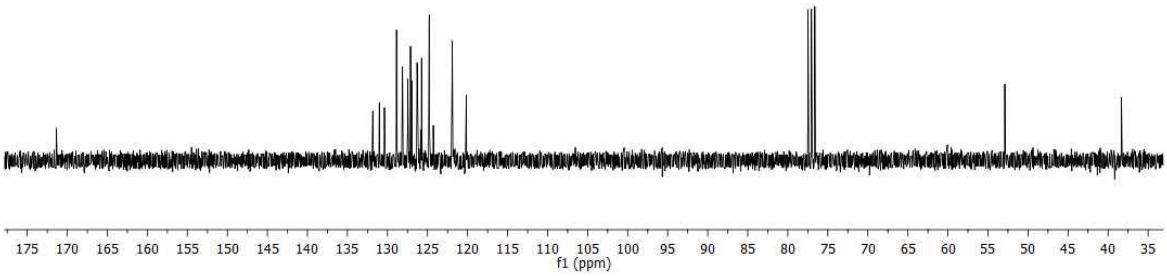

S2.3 ^{1}H NMR and $^{13}C\{^{1}H\}$ spectra of complex **4** in $CDCl_3$

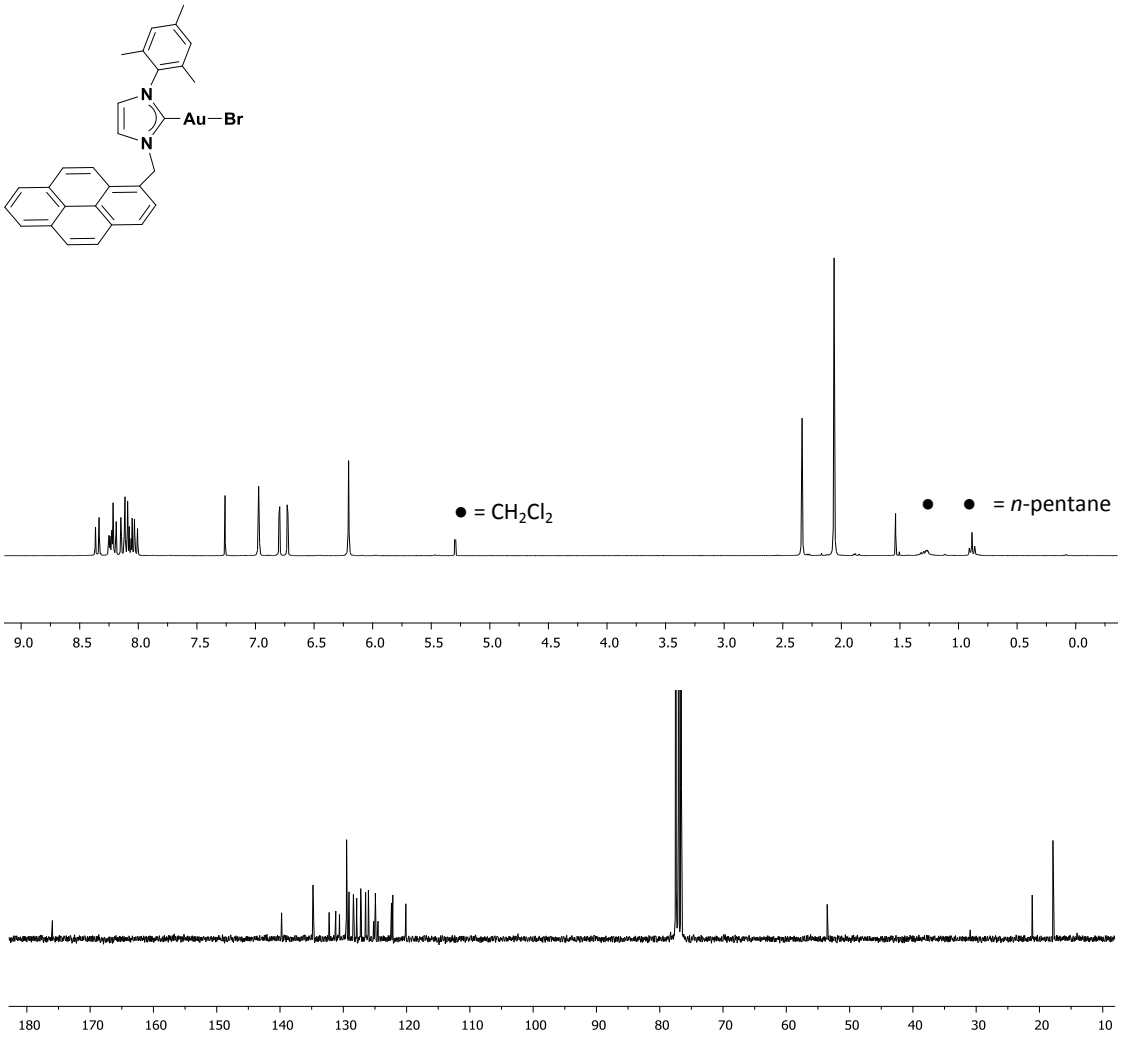

S2.4 ^{1}H NMR of isolated 2-phenyl-1H-indole and 2-n-butyl-1H-indole

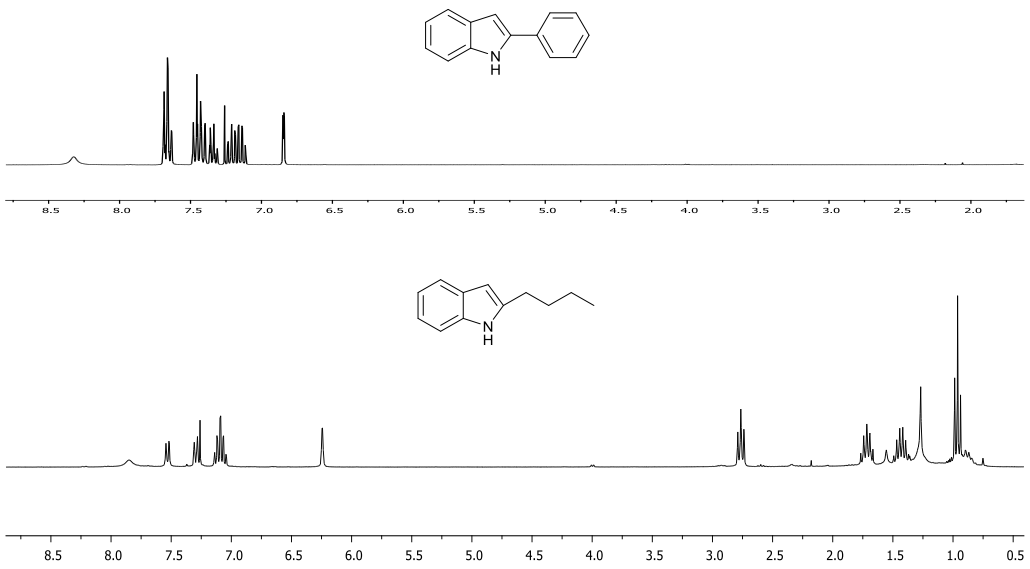

S3. High Resolution Mass Spectroscopy (HRMS)

S3.1 HRMS of complex **3**

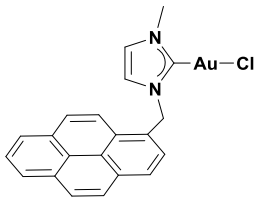

MW = 528.7847 g/mol

Fragment: 567.0309 $[M + K]^+$

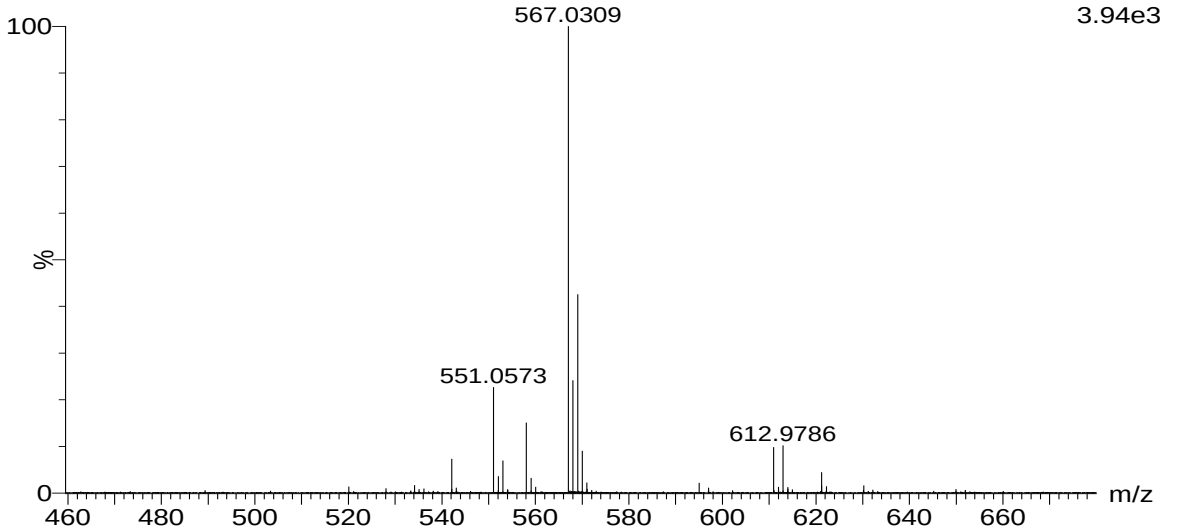

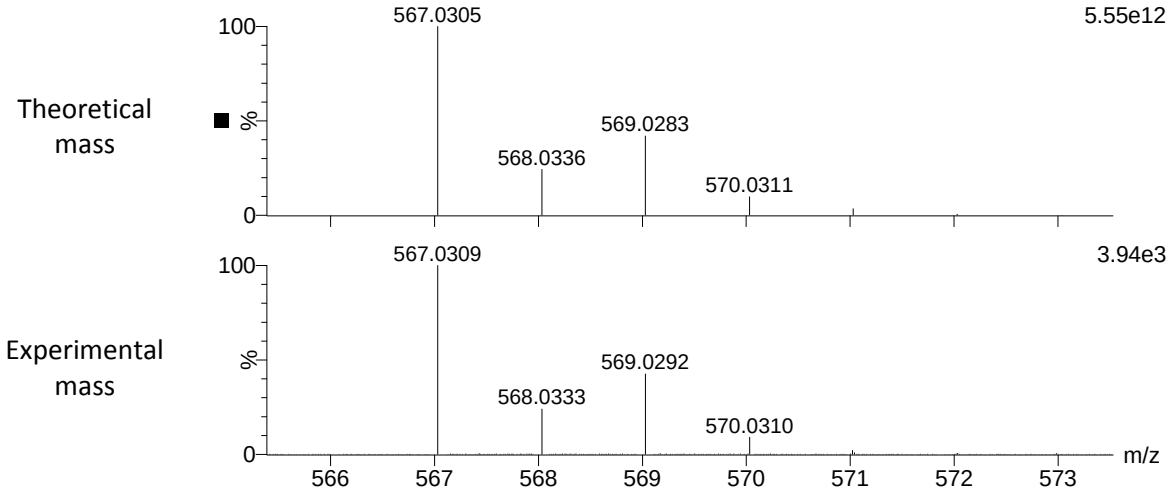

Peak (m/z)	Experimental mass	Theoretical mass	Relative error (ppm)
567.0	567.0309	567.0305	0.7

S3.2 HRMS of complex 4

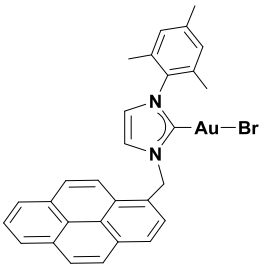

MW = 528.7847 g/mol

Fragment: 763.0305 $[M - Br + I + K]^+$

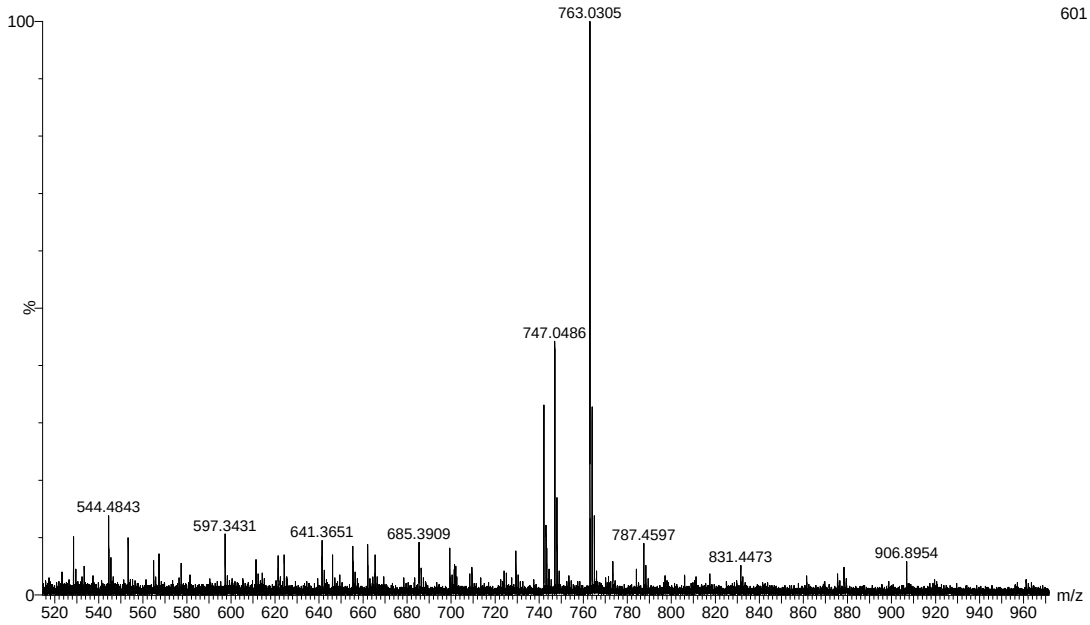

Theoretical mass

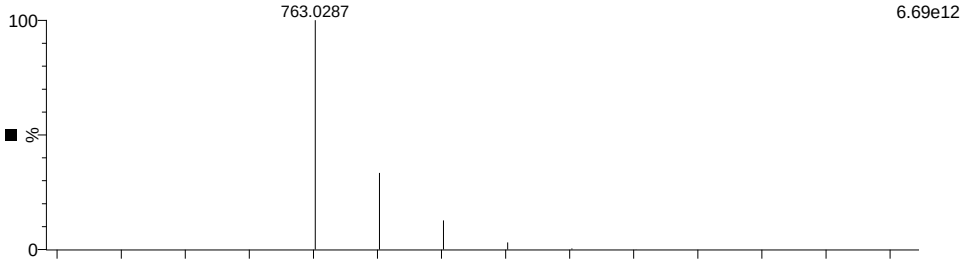

Experimental mass

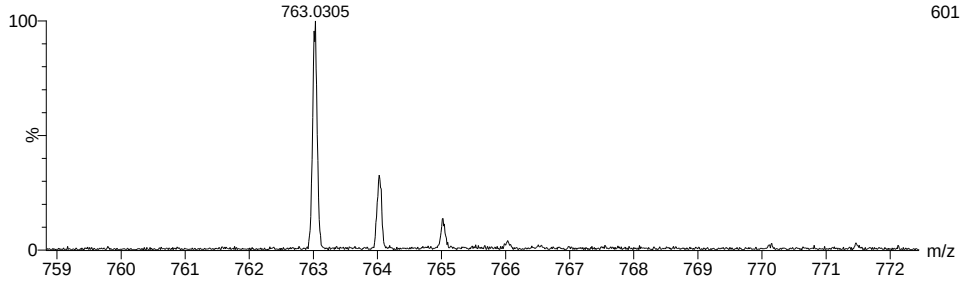

Peak (m/z)	Experimental mass	Theoretical mass	Relative error (ppm)
763.0	763.0305	763.0287	2.4

S4. Single crystal X-ray Diffraction Studies

S4.1 Crystal data of complex 3

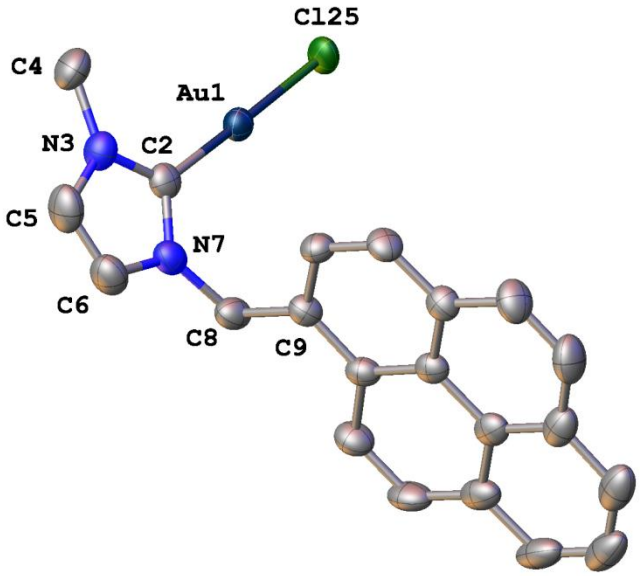

Molecular diagram of complex **3**

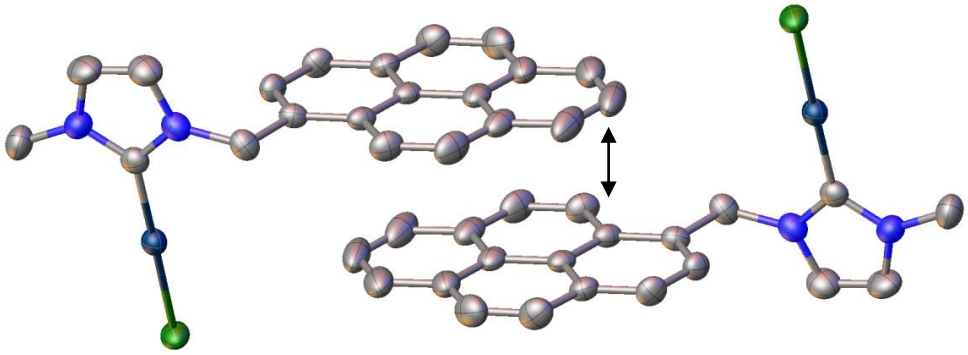

Packing diagram of complex **3** showing an interplanar distance between the pyrenes of 3.5 Å.

Table S2 Crystal data and structure refinement for complex 3.

Identification code	str1609
Empirical formula	$C_{21}H_{16}AuClN_2$
Formula weight	528.77
Temperature/K	200.00(10)
Crystal system	monoclinic
Space group	$P2_1/c$
a/Å	12.2750(3)
b/Å	11.5743(3)
c/Å	12.3319(3)
α/°	90
β/°	96.802(2)
γ/°	90
Volume/Å^3	1739.71(7)
Z	4
ρ_{calc}g/cm^3	2.019
μ/mm^{-1}	8.615
F(000)	1008.0
Crystal size/mm^3	0.12 × 0.1 × 0.09
Radiation	MoKα (λ = 0.71073)
2Θ range for data collection/°	5.656 to 51.998
Index ranges	-15 ≤ h ≤ 15, -14 ≤ k ≤ 14, -15 ≤ l ≤ 15
Reflections collected	33714
Independent reflections	3420 [R_{int} = 0.0338, R_{sigma} = 0.0160]
Data/restraints/parameters	3420/0/275
Goodness-of-fit on F^2	1.066
Final R indexes [I>=2σ (I)]	R_1 = 0.0210, wR_2 = 0.0563
Final R indexes [all data]	R_1 = 0.0253, wR_2 = 0.0590
Largest diff. peak/hole / e Å^{-3}	1.09/-0.42

S4.2 Crystal data of complex 4

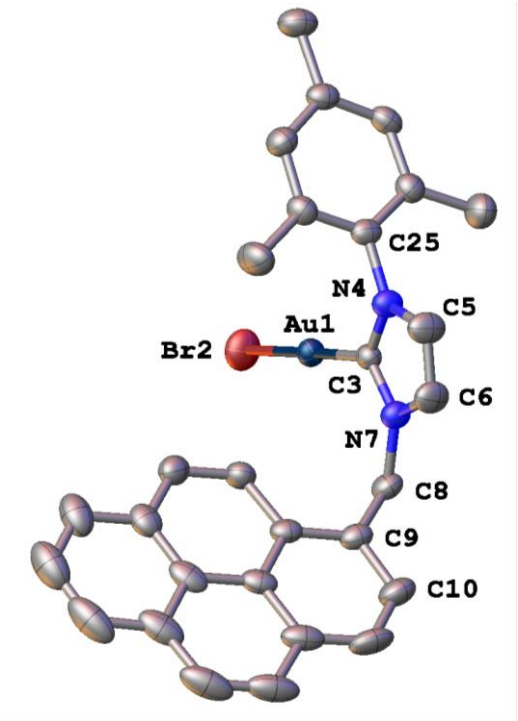

Molecular diagram of complex **4**

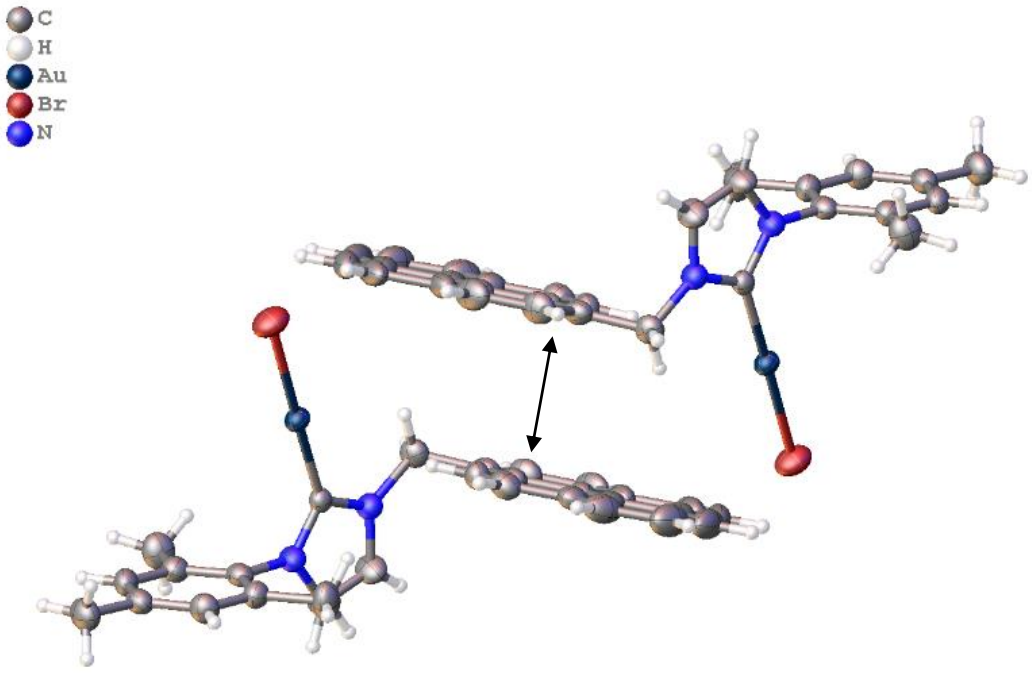

Packing diagram of complex **4** showing an interplanar distance between the pyrenes of 3.6 Å.

Table S3 Crystal data and structure refinement for complex **4.**

Identification code	str1873
Empirical formula	$C_{29}H_{24}AuBrN_2$
Formula weight	677.38
Temperature/K	199.95(10)
Crystal system	triclinic
Space group	P-1
a/Å	9.90077(15)
b/Å	10.88818(19)
c/Å	11.9329(2)
α/°	87.9710(14)
β/°	86.3634(13)
γ/°	71.0433(15)
Volume/Å^3	1214.01(4)
Z	2
ρ_{calc}g/cm^3	1.853
μ/mm^{-1}	7.724
F(000)	652.0
Crystal size/mm^3	0.288 × 0.204 × 0.124
Radiation	MoKα (λ = 0.71073)
2Θ range for data collection/°	5.686 to 52.742
Index ranges	-12 ≤ h ≤ 12, -13 ≤ k ≤ 13, -14 ≤ l ≤ 14
Reflections collected	48631
Independent reflections	4946 [R_{int} = 0.0494, R_{sigma} = 0.0226]
Data/restraints/parameters	4946/0/301
Goodness-of-fit on F^2	1.071
Final R indexes [I>=2σ (I)]	R_1 = 0.0221, wR_2 = 0.0530
Final R indexes [all data]	R_1 = 0.0248, wR_2 = 0.0543
Largest diff. peak/hole / e Å^{-3}	0.99/-0.76

S5. Characterization of the hybrid materials

S5.1 FTIR Spectroscopy

Infrared spectra (FTIR) were performed on a JASCO FT/IR-6200spectrometer with a spectral window of 4000-500 cm^{-1}. The samples were prepared as KBr disks.

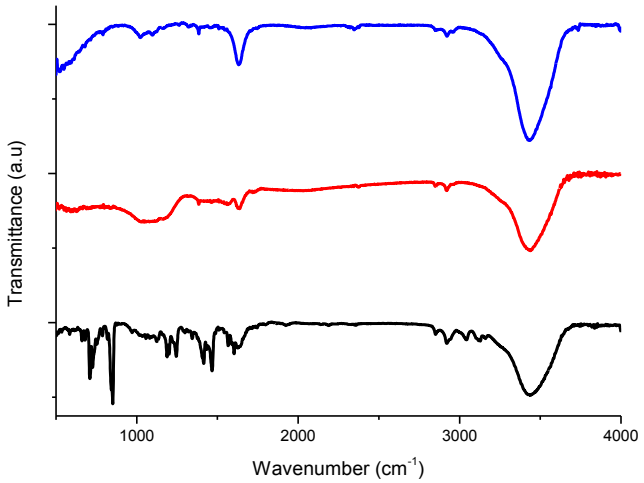

Figure S1. FTIR spectra of rGO (blue), gold complex **3** (black) and the hybrid material **5** (red).

S5.2 UV/Vis spectroscopy.

The UV/Vis spectra were recorded between 250 and 600 nm by a Cary 300 Bio UV−Vis Varian spectrophotometer. The samples were suspended in DMF and sonicated for 5 minutes before the measurements. The molecular complexes were dissolved in DMF (10^{-6}M).

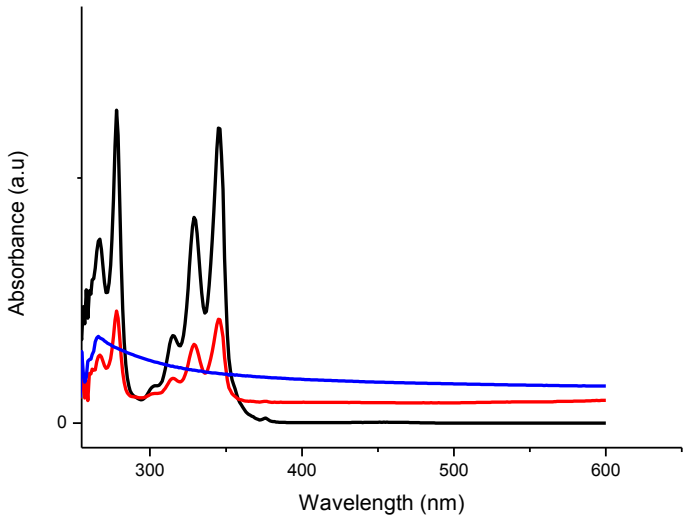

Figure S2. UV/Vis of rGO (blue), gold complex **3** (black) and the hybrid material **5** (red).

S6. High Resolution Transmission Electron Microscopy (HRTEM) images

High-resolution images of transmission electron microscopy HRTEM and high-angle annular dark-field HAADF-STEM images of the samples were obtained using a Jem-2100 LaB6 (JEOL) transmission electron microscope coupled with an INCA Energy TEM 200 (Oxford) energy dispersive X-Ray spectrometer (EDX) operating at 200 kV. Samples were prepared by drying a droplet of a MeOH dispersion on a carbon-coated copper grid.

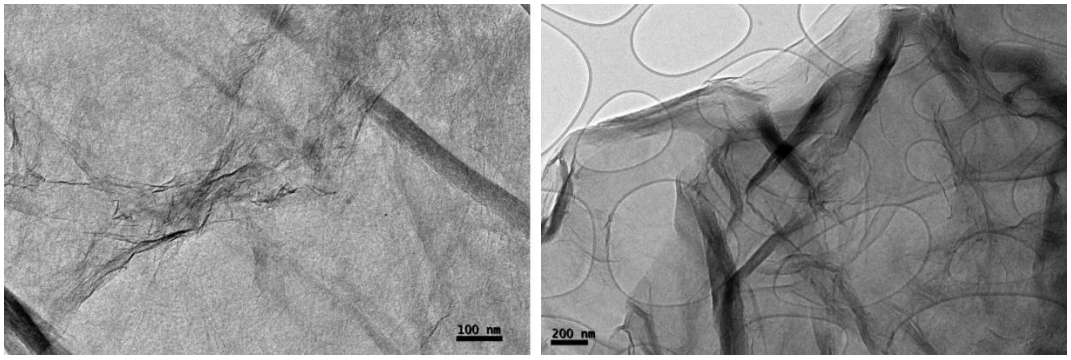

Figure S3. HRTEM images of the hybrid material **5**

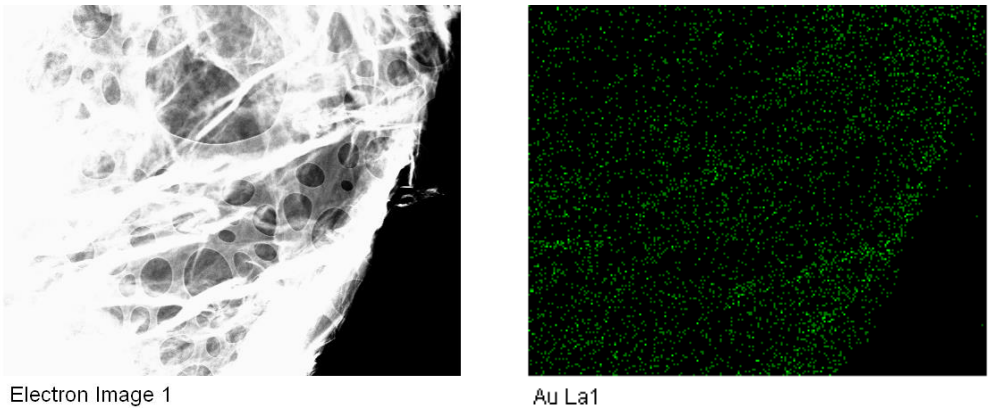

Figure S4. STEM image of the hybrid material **5** (left) and EDS elemental mapping image showing the homogeneous distribution of gold (right).

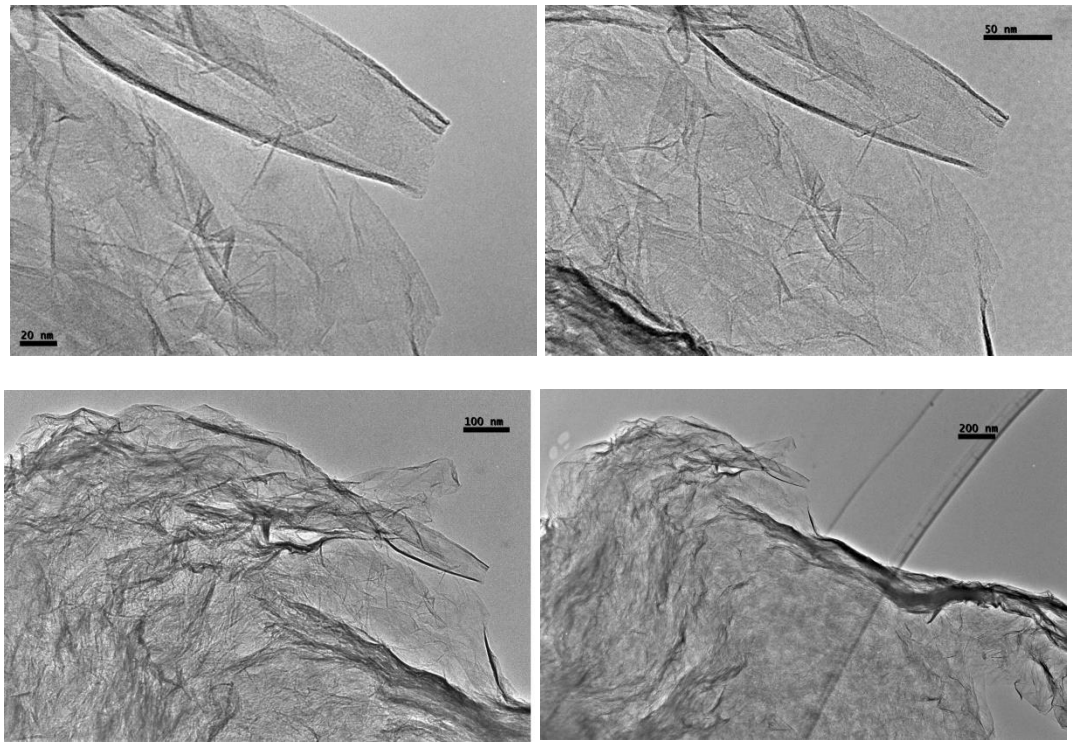

Figure S5. HRTEM images of the hybrid material **6**

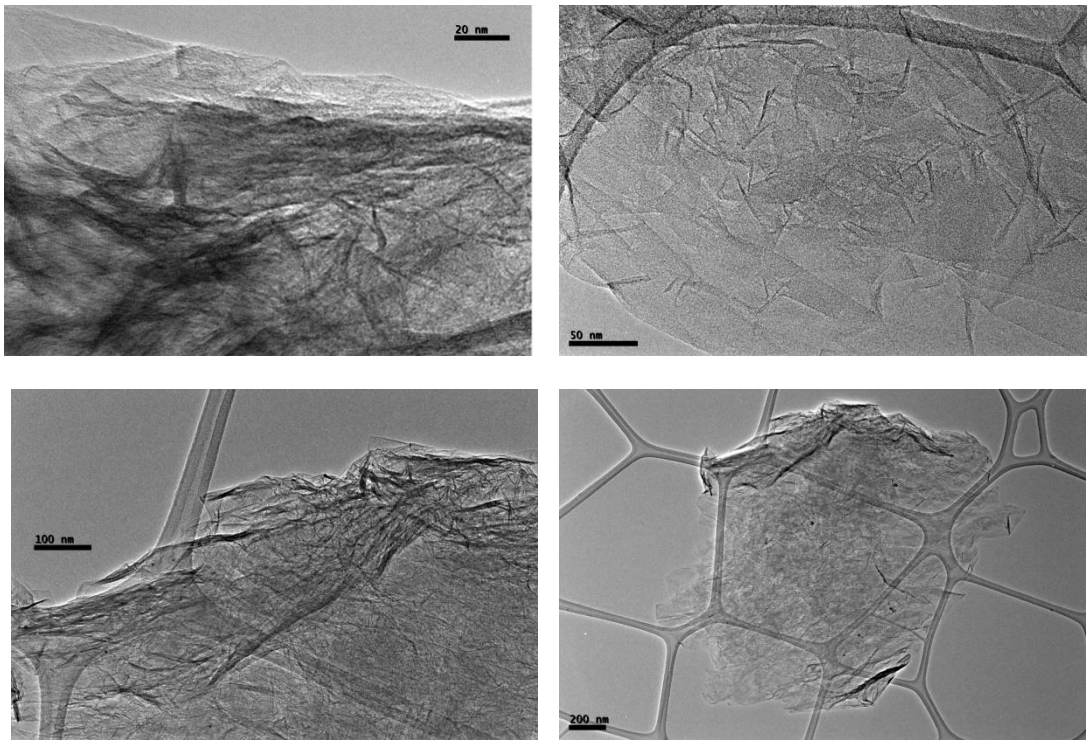

Figure S6. HRTEM images of the hybrid material **6** after six catalytic cycles

S7. X-ray Photoelectron Spectroscopy (XPS)

X-ray photoelectron spectroscopy (XPS) spectra were acquired on a Kratos AXIS ultra DLD spectrometer with a monochromatic Al Kα X-ray source (1486.6 eV) using a pass energy of 20 eV. The photoelectron take off angle was 90^{o} with respect to the sample plane. To provide a precise energy calibration, the XPS binding energies were referenced to the C1s peak at 284.6 eV.

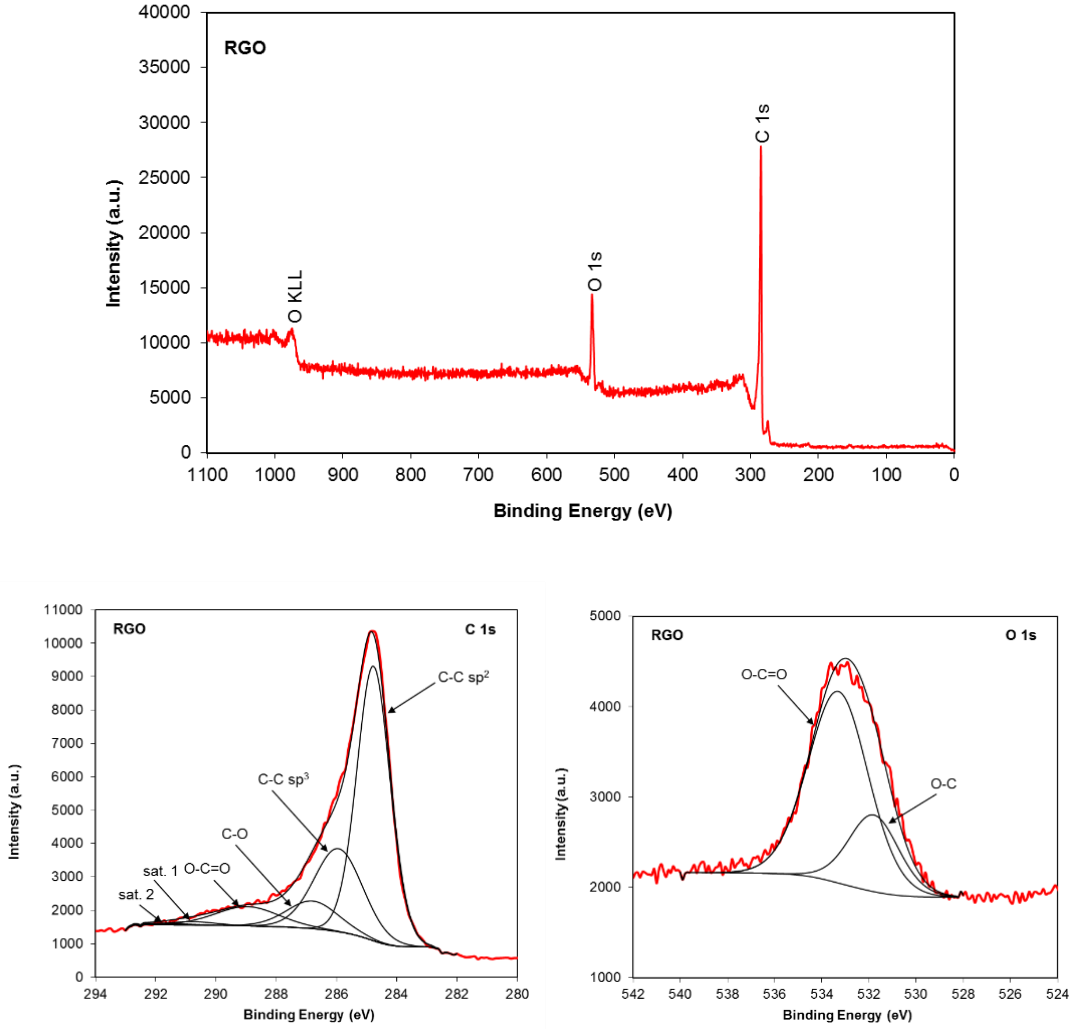

Figure S7. XPS survey scan of **rGO** and high resolution of C1s and O1s core-levels.

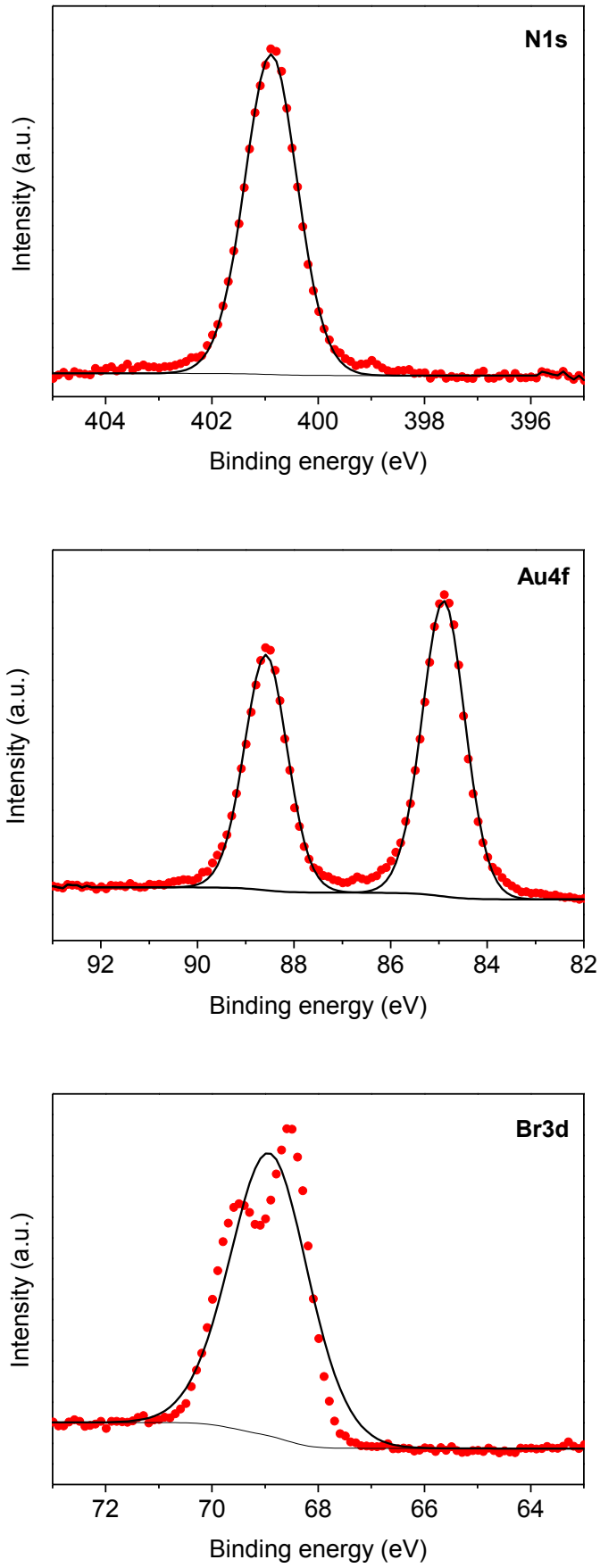

Figure S8. XPS of **4** showing the high resolution N1s, Au4f and Br3d core-levels.

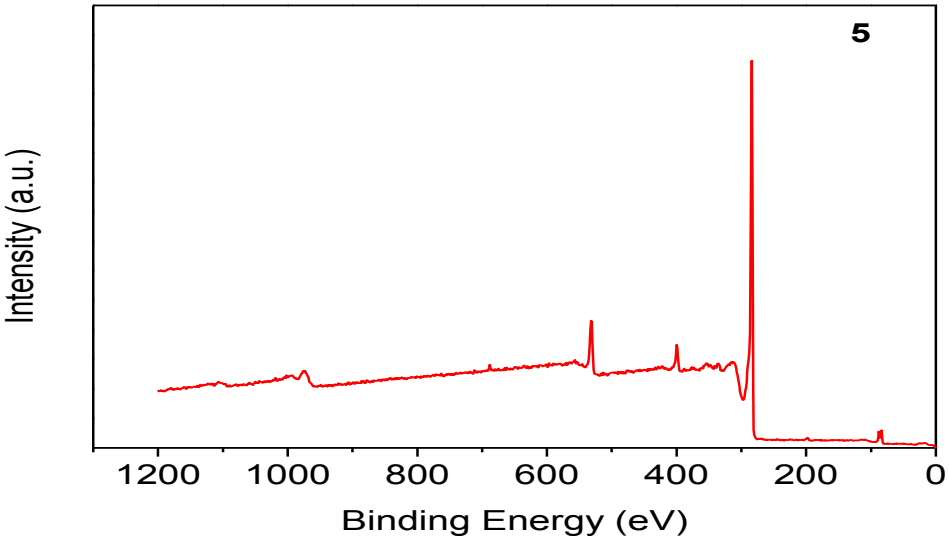
5
Intensity (a.u.)
1200
1000
800
600
400
200
0
Binding Energy (eV)

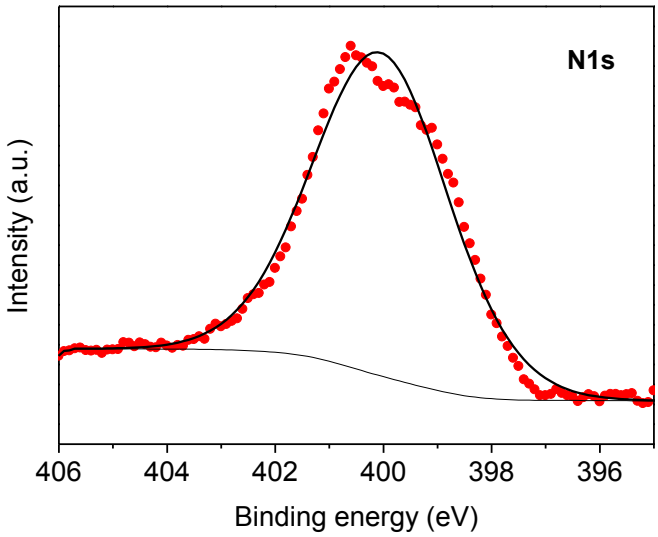
N1s
Intensity (a.u.)
406
404
402
400
398
396
Binding energy (eV)

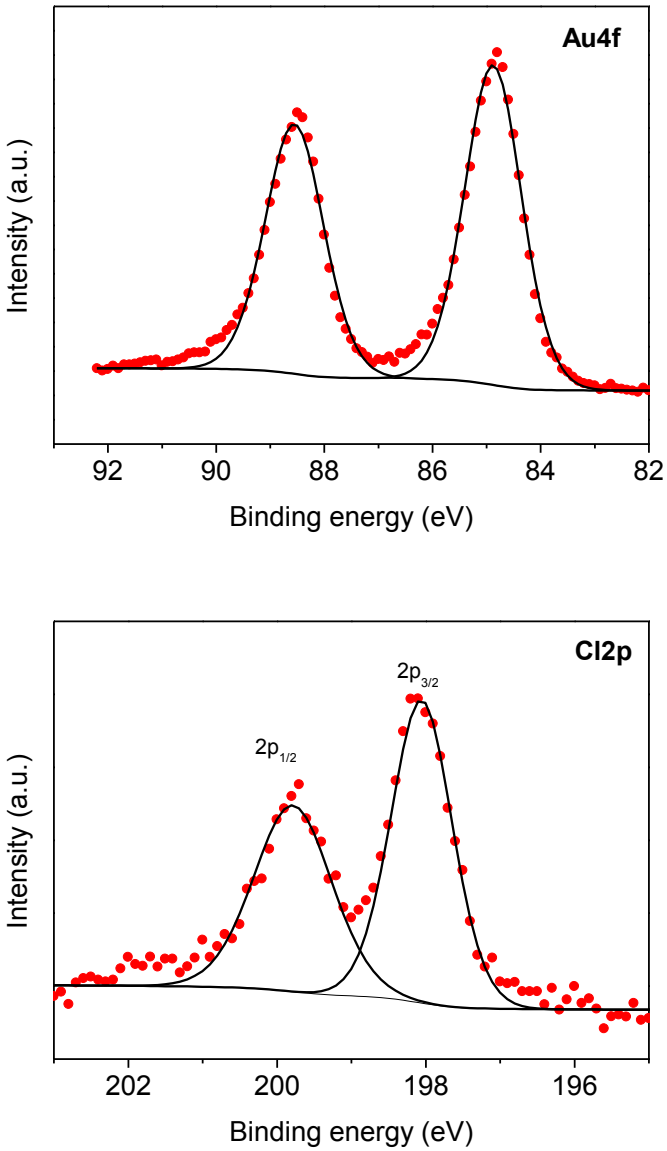

Figure S9. XPS survey scan of **5** and high resolution of N1s, Au4f and Cl2p core-levels.

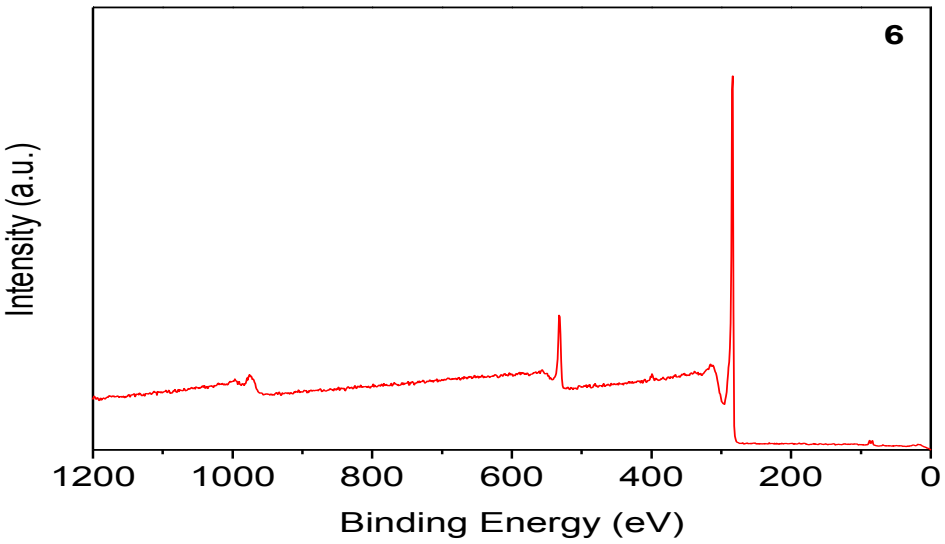
6
Intensity (a.u.)
1200
1000
800
600
400
200
0
Binding Energy (eV)

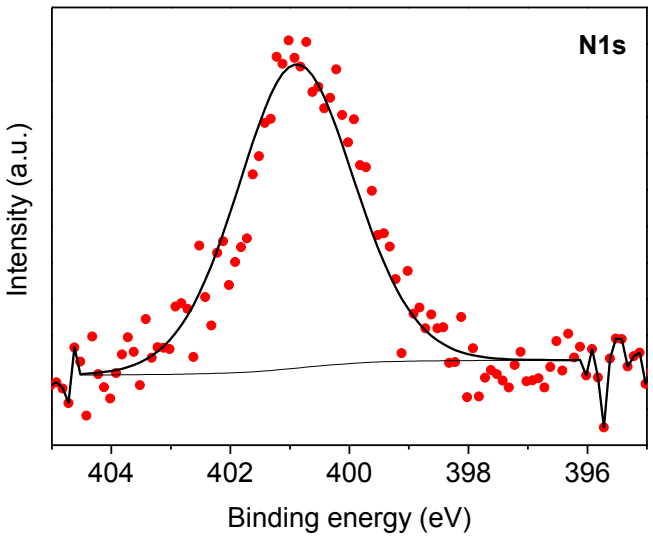
N1s
Intensity (a.u.)
404
402
400
398
396
Binding energy (eV)

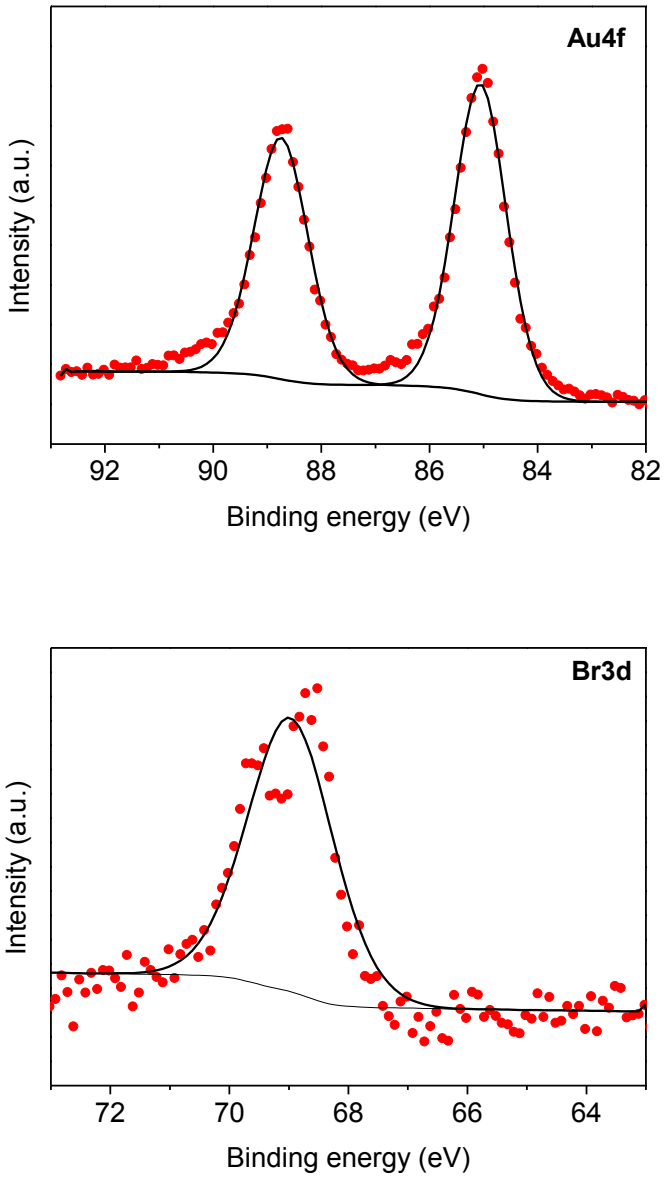

Figure S10. XPS survey scan of **6** and high resolution of N1s, Au4f and Br3d core-levels.